CHEMISTRY
AN ASIAN JOURNAL
www.chemasianj.org

Accepted Article

Title: The Quest of Excited-State Intramolecular Proton Transfer via Eight-Membered Ring π-Conjugated Hydrogen Bonding System

Authors: Fan-Yi Meng, Yen-Hao Hsu, Zhiyun Zhang, Pei-Jhen Wu, Yi-Ting Chen, Yi-An Chen, Chi-Lin Chen, Chi-Min Chau, Kuan-Miao Liu, and Pi-Tai Chou

To be cited as: *Chem. Asian J.* 10.1002/asia.201701057

Link to VoR: http://dx.doi.org/10.1002/asia.201701057

A Journal of

ACES
Asian Chemical Editorial Society

A sister journal of **Angewandte Chemie** and **Chemistry – A European Journal**

WILEY-VCH

10.1002/asia.201701057

WILEY-VCH

FULL PAPER

The Quest of Excited-State Intramolecular Proton Transfer via Eight-Membered Ring π-Conjugated Hydrogen Bonding System

Fan-Yi Meng,[a]§ Yen-Hao Hsu,[a]§ Zhiyun Zhang,*[a] Pei-Jhen Wu,[a] Yi-Ting Chen,[a] Yi-An Chen,[a] Chi-Lin Chen,[a] Chi-Min Chao,[b] Kuan-Miao Liu,[b] and Pi-Tai Chou*[a]

Dedication ((optional))

Abstract: Searching for eight-membered ring π-conjugated hydrogen bonding (8-MR H-bonding) systems with excited-state intramolecular proton transfer (ESIPT) property is seminal and synthetically challenging. In this work, a series of π-conjugated molecules (**8-HB-1**, **8-HB-L1** and **8-HB-2**) potentially possessing 8-MR H-bond are strategically designed, synthesized and characterized. The configurations of these three potential molecules are checked by their X-ray structures, among which **8-HB-L1** (a structurally locked **8-HB-1** core chromophore) is proved to be an 8-MR H-bonding system, whereas **8-HB-1** and **8-HB-2** are too sterically hindered to form the 8-MR intramolecular H-bond. The ESIPT property of **8-HB-L1** is confirmed by the dual fluorescence consisting of normal and proton-transfer tautomer emissions. The insight into the ESIPT process of **8-HB-L1** is provided by femtosecond fluorescence upconversion measurements together with computational simulation. The results demonstrate for the first time a successful synthetic route to attain an 8-MR H-bonding molecule **8-HB-L1** with ESIPT property.

Introduction

Searching for a new type of π-conjugated intramolecular hydrogen bonding (H-bonding) system associated with unique photophysical properties such as the excited-state intramolecular proton transfer (ESIPT) reaction is always important and fascinating.[1] Herein we define the π-conjugated H-bond as the H-bonding from which the switch of proton from donor to acceptor site may induce the π-electron rearrangement and hence the delocalization of the π-conjugation. Vice versa, the H-bond properties may be affected by the redistribution of the π electrons induced by electronic excitation, resulting in the proton relocation, i.e., ESIPT, forming a proton transfer tautomer.

Most intramolecular H-bonding systems involve hydroxyl or pyrrolic proton (–OH or –NH) as the proton donor while carbonyl oxygen or pyridyl nitrogen serves as an acceptor.[1] Along this line, a representative for five-membered ring (5-MR) intramolecular H-bond can be ascribed to 3-hydroxyflavone[2] or 2-pyridylpyrazole,[3] forming C=O···H–O and N···H–N H-bond, respectively, from which ESIPT takes place. Relative to the absorption peak wavelength, the resulting proton-transfer tautomer exhibits anomalously large Stokes shifted emission that is pertinent for potential optoelectronic and sensing applications.[4] Upon increasing the H-bonding size, the six-membered ring (6-MR) H-bonding systems are more common,[5],[6],[7],[8] the favorable geometry of which leads to a rather strong hydrogen bond and hence a shorter H-bonding distance, driving a fast ESIPT. Prototypical examples are methylsalicylate,[5] 10-hydroxybenzoquinoline,[6] 2-hydroxybenzo-thiazole[7] and 7-(2′-pyridyl)indole,[8] covering various different types of H-bond.

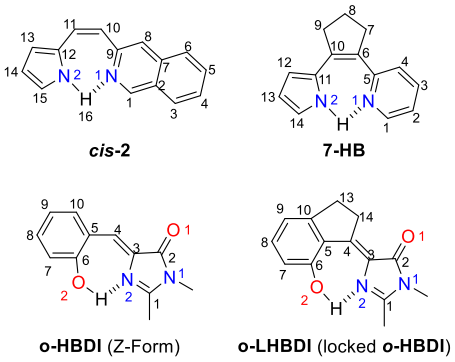

Scheme 1. The representative seven-membered ring (7-MR) H-bonding systems with ESIPT.

It then becomes obscure when the π-conjugated H-bonding system is greater than 6-MR. Needless to say that the system is designated to undergo ESIPT. To our best knowledge, the first seven-membered ring (7-MR) H-bonding system undergoing ESIPT should be ascribed to the *cis*-1-(2-pyrrolyl)-2-(2-quinolyl)ethane (***cis*-2**, Scheme 1).[9] Another example is an ortho-GFP core chromphore[10] (***o*-HBDI**, Scheme 1), which is stable as a *Z*-form, possessing a 7-MR intramolecular H-bond between –OH and immidazole nitrogen. Upon electronic excitation (~400 nm), ***o*-HBDI** undergoes intramolecular proton transfer, resulting in a large Stokes shifted tautomer emission at 605 nm. Recently,

[a] F.-Y. Meng,§ Y.-H. Hsu,§ Dr. Z. Zhang, P.-J. Wu, Y.-T. Chen, Y.-A. Chen, C.-L. Chen, Prof. P.-T. Chou
Department of Chemistry
National Taiwan University
Taipei, 10617, Taiwan, R.O.C.
E-mail: zhangzhiyun@hotmail.com
chop@ntu.edu.tw
[b] Prof. C.-M. Chao, Prof. K.-M. Liu
Department of Medical Applied Chemistry and Department of Medical Education
Chung Shan Medical University
Taichung, 40201, Taiwan, R.O.C.
§These authors contributed equally

Supporting information for this article is given via a link at the end of the document.((Please delete this text if not appropriate))

10.1002/asia.201701057

we have reported a structurally locked ***o*-HBDI** core chromophore, ***o*-LHBDI**[11] (Scheme 1). Owing to the inherent inhibition of rotational motion, ***o*-LHBDI** rendered an intense tautomer emission capable of generating amplified spontaneous emission via four electronic levels. Subsequently, another prototype (**7-HB**,[8b] see Scheme 1) possessing 7-MR pyridine-pyrrole H-bond has also been reported to exhibit ESIPT property.

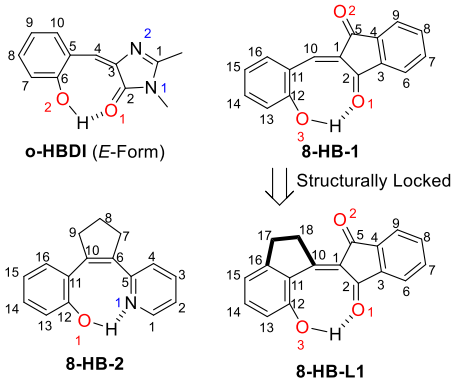

Scheme 2. The proposed potential eight-membered ring (8-MR) H-bonding systems with ESIPT.

For further extension, it is then of great interest to search for any eight-membered ring (8-MR) intramolecular H-bonding systems endowed with ESIPT property. Theoretically, the 8-MR H-bonded systems can effectively extend the π-conjugated length and may thus serve as a case in point to develop deep-red and near infrared fluorescent materials by exploiting the anomalously large Stokes shifted tautomer emission. The 8-MR intramolecular H-bond can be easily realized in the flexible chain molecules, such as peptides of aminoxy acids as foldamers.[12] However, development of π-conjugated molecules with 8-MR intramolecular H-bond is of great challenge, which, to our knowledge, is unprecedented. From the viewpoint of chemical structure, we first mulled over the *E* isomer of ***o*-HBDI** (Scheme 2) as a case in point, which shows an 8-MR, C(2)=O(1)···H–O(2) H-bonding configuration. Unfortunately, due to the steric hindrance and weaker H-bond, the *E* isomer is thermally unfavorable compared with that of the *Z* form (see Scheme 1).[13] To lift the *E*,*Z*-restriction, we then utilized the 1*H*-indene-1,3(2*H*)-dione to replace the imidazole moiety of ***o*-HBDI,** and synthesized a potential 8-MR H-bonding molecule, 2-(2-hydroxybenzylidene)-1*H*-indene-1,3(2*H*)-dione (**8-HB-1**) (Scheme 2). In yet another approach, inspired by **7-HB** (Scheme 1), we utilized phenol to replace the pyrrole moiety and strategically designed and synthesized another potential 8-MR H-bonding system 2-(2-(pyridin-2-yl)cyclopent-1-enyl)phenol (**8-HB-2**) (Scheme 2). Unfortunately, further crystal structure investigations of **8-HB-1** and **8-HB-2** were found to lack intramolecular H-bond (*vide infra*). To ascertain the 8-MR H-bonding π-conjugated system, we then intentionally locked the free rotational single bond C10−C11 of **8-HB-1** with the 2-phenol ring, yielding the third potential 8-MR H-bonding molecule 7-hydroxy-2,3-dihydro-[1,2'-biindenylidene]-1',3'-dione (**8-HB-L1**) (Scheme 2). Details of results and discussion are elaborated below.

Results and Discussion

Synthesis

As depicted in Scheme 3a, with a green synthetic methodology,[14] **8-HB-1** could be obtained by reacting 1*H*-indene-1,3(2*H*)-dione (**ID**) and 2-hydroxybenzaldehyde in water. However, a similar protocol using **ID** and 7-hydroxy-1-indanone (**7-HI**) as the starting material in an attempt to synthesize **8-HB-L1** unfortunately failed (see Scheme 3b, route 1). Amid the reaction, monitored by the thin-layer chromatography (TLC), the result showed that **7-HI** remained intact while **ID** disappeared. With a harsher approach, we then used $TiCl_4$ (in THF) to chelate the carbonyl oxygen of **7-HI**, which should increase the neucleophilicity of **7-HI** and thus facilitates the condensation reaction (see Scheme 3b, Route 2). This modification was unsuccessful either. Alternatively, we then reacted **7-HI** with $PhNH_2$ in the presence of catalytic formic acid to form the Schiff-base type precursor (*E*)-3-(phenylimino)-2,3-dihydro-1*H*-inden-4-ol (**PDI**) (Scheme 3b, Route 3). Schiff base has been commonly used as a base for deprotonation via the formation of an iminium cation that facilitates the reactivity of nucleophicity of C=N. As expected, **PDI** reacted with **ID** in acetonitrile successfully, affording **8-HB-L1** with a moderate yield (33%). In yet a separated route (Scheme 3c), 1,2-dibromocyclopent-1-ene was used as the starting material, which was then coupled with (2-methoxyphenyl)boronic acid and 2-(tributylstannyl)pyridine by sequential Suzuki and Stille couplings, followed by demethoxylation with BBr_3 in CH_2Cl_2, to form another potential 8-MR H-bonding system, **8-HB-2**. All new compounds were fully verified with ^{1}H NMR, ^{13}C NMR and HRMS, and detail of synthetic route is elaborated in the Experimental Section.

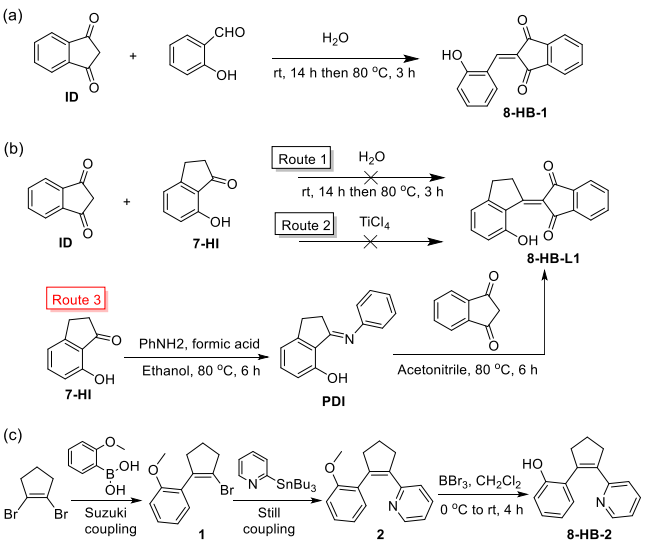

Scheme 3. Synthetic routes of the titled compounds.

10.1002/asia.201701057

Crystal Structures

Chemically, under the same proton donating and accepting strength, the more planar H-bonding configuration should result in a stronger H-bond. Accordingly, nearly planar H-bonding geometry was frequently found in 5- and 6-MR H-bonding systems and was also recently confirmed in the 7-MR H-bonding cases.[10] Extending to 8-MR H-bonding configuration, simple maneuver on the geometry constraint indicates that the formation of a planar 8-MR H-bonding is nontrivial. For example, we anticipated that **8-HB-1** and **8-HB-2** may potentially form planar 8-MR H-bond. Conversely, as shown in the X-ray structure (see Figure 1a for **8-HB-1**), apart from the 8-MR H-bonding configuration drawn in Scheme 2, the phenol ring of **8-HB-1** rotates ~171° (∠C12–C11–C10–C1) along the C10–C11 single bond that serves as the linker for the proton donor and acceptor aryl rings. It is also noteworthy that **8-HB-1** takes a nearly planar structure, with a small torsional angle of 6.2° (∠C11–C10–C1–C2). On the one hand, this nearly planar structure without involving intramolecular H-bond is believed to result from the strong electron push-pull interactions together with two intermolecular O–H···O H-bonds in a dimeric formation (Figure 1c). On the other hand, careful examination of the crucial bond angles of **8-HB-1** indicates that both ∠O3–C12–C11 and ∠C12–C11–C10 are around 117° (Table 1), which is much smaller than 135°, a theoretical interior angle calculated for a regular polygon with eight sites. The result implies the difficulty to overcome the steric hindrance upon forming the 8-MR intramolecular H-bond in a flexible structure such as **8-HB-1**. The steric hindrance of 8-MR intramolecular H-bonding formation is even larger for **8-HB-2**. The X-ray structure of **8-HB-2**, shown in Figure S1 in Supporting Information, reveals two twisted isomers with different torsional angles, forming two types of intermolecular O−H···N H-bonding arrangement in the crystal lattice (Figure S2 in Supporting Information). Obviously, all bond angles involved in the potential H-bonding formation are substantially smaller than 135° (see Table S1 in Supporting Information for detail), rationalizing its lack of intramolecular H-bonding formation.

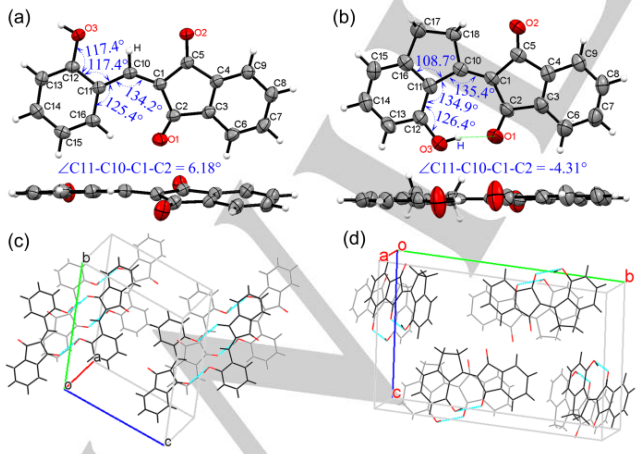

Figure 1. Single crystal structures of (a) **8-HB-1** and (b) **8-HB-L1**: the top images show a front view of the structures and the bottom pictures show the side-view to illustrating the planarity of the structures. Overlap packing of (c) 8-HB-1 and (d) 8-HB-L1 with the cell axes.

Upon locking the C10–C11 bond of **8-HB-1,** forming **8-HB-L1**, the C(2)=O(1)···H–O(3) 8-MR intramolecular H-bonding configuration was then firmly evidenced by its crystal structure (Figure 1b), in which C10 and C16 are linked by the ethane bridge (C17–C18). This brings two advantages for forming the 8-MR H-bond. Firstly, the rotation of C10–C11 is inhibited due to its lock with the phenol ring. Secondly, as listed in Table 1, the ∠C16–C11–C10 angle is much reduced from ~125° in **8-HB-1** to ~108° in **8-HB-L1**, and correspondingly ∠C12–C11–C10 angle is increased from ~117° in **8-HB-1** to ~135° in **8-HB-L1**. Nevertheless, the steric hindrance cannot be completely suppressed, such that the corresponding H-bonding geometry for **8-HB-L1** is not fully planar, evidenced by the torsional angle of ∠C11–C10–C1–C2 ~4.3° (Figure 1b and Table 1), which is larger than that in 7-MR H-bonding systems such as ***o*-HBDI** (∠C5−C4−C3−N2 ~1.5°)[10] and ***o*-LHBDI** (~0°)[11] (see Scheme 1 and Figure S3 in Supporting Information). The H-bonding distance in the C(2)=O(1)···H–O(3) 8-MR configuration of **8-HB-L1** is measured to be as short as 1.583 Å via X-ray analyses. Accordingly, whether ESIPT can take place in **8-HB-L1** is of great interest.

Table 1. The Values of Selected Angles in Crystal Structures of **8-HB-1** and **8-HB-L1**

Selected Angles	8-HB-1	8-HB-L1
∠O3−C12−C11	117.4°	126.4°
∠C12−C11−C10	117.4°	134.9°
∠C11−C10−C1	134.2°	135.4°
∠C10−C1−C2	133.5°	132.2°
∠C1−C2−O1	129.2°	130.4°
∠C2−O1−H	-	114.8°
∠O1−H−O3	-	195.8°
∠H−O3−C12	-	109.5°
∠C16−C11−C10	125.4°	108.7°
∠C11−C10−C1−C2	6.2°	-4.3°
∠C12−C11−C10−C1	-171.1°	-1.7°

ESIPT Property

Figure 2 shows optical properties of **8-HB-L1** in cyclohexane (red line), in which the absorption spectrum displays an intense peak at 364 nm. Upon excitation (e.g. 350 nm) **8-HB-L1** displays a rather weak emission band maximized at 490 nm, accompanied by a second band appearing at ~700 nm (see Figure 2). The overall dual-band emission yield was estimated to be as low as (2.2±0.5) x 10^{-5} in cyclohexane. In comparison, non-H-bonded **8-HB-1** is considered to be a non-proton transfer prototype, which shows a single emission band maximized at ~475 nm (see black line in Figure 2) with a low emission yield of (4.3±0.5) x 10^{-5}. On the basis of time-dependent DFT (B3LYP/6-31+G(d,p)) with geometry optimization of **8-HB-L1** in the ground state, the $S_0 \rightarrow S_1$ was calculated to be 420 nm. The geometry optimization of the S_1

10.1002/asia.201701057

state always relaxes to the proton-transfer tautomer S'_1 state (prime sign denotes the tautomer), indicating that a rather small or even negligible barrier for ESIPT of **8-HB-L1**. The vertical $S'_1 \rightarrow S'_0$ transition of the proton-transfer tautomer is calculated to be 1.56 eV (793 nm, see Figure 3). As a result of calculation, ESIPT is thermodynamically favorable by ~18 kcal/mol in cyclohexane (see Figure 3). This value is considered to be an upper limit of the energy difference because the optimized S_1 state cannot be obtained under current computational level. The matched experimental and computational data supports the occurrence of ESIPT in **8-HB-L1** in cyclohexane, giving normal (490 nm) and proton-transfer tautomer (700 nm) emission bands. It's deserved to mention that the tautomeric emission band ~700 nm is located at the region of near infrared emission. The steady-state optical properties of **8-HB-L1** *and* **8-HB-1** were also investigated in dichloromethane (polar aprotic solvent) and *tert*-butyl alcohol (polar protic solvent). As shown in Figure S3 in Supporting Information, the absorption spectra of **8-HB-L1** in various solvents are almost identical. Unlike the resolvable dual emission in cyclohexane, the tautomer band of **8-HB-L1** cannot be well resolved in dichloromethane because of the relatively week tautomer emission. Similar to a number of ESIPT dyes in protic solvents, **8-HB-L1** only showed normal emission in *tert*-butyl alcohol plausibly due to the stronger intermolecular H-bonding formation that ruptures the weak intramolecular H-bond. As shown in Figure S4, **8-HB-1** exhibited more obvious charge transfer absorption band (~400 to 500 nm) from nonpolar cyclohexane to polar *tert*-butyl alcohol as well as small red-shifted emission. Also note that **8-HB-2** is virtually non-emissive in various solvents, due perhaps to the much flexible molecular structure that induces drastic nonradiative quenching.

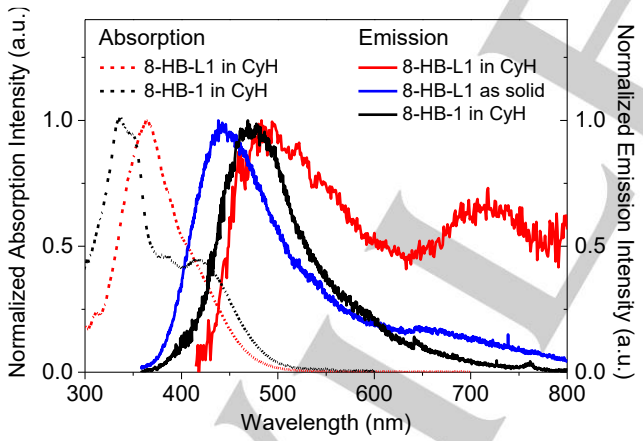

Figure 2. The normalized absorption (red dash) and emission (red solid) spectra of **8-HB-L1** in cyclohexane (CyH) as well as emission spectrum in solid state (blue solid). Also shown are the absorption (black dash) and emission (black solid) spectra of **8-HB-1** in cyclohexane. λ_{ex} = 355 nm. A > 400 nm band passed filter was inserted in front of the emission monochromator to eliminate the second-order signal.

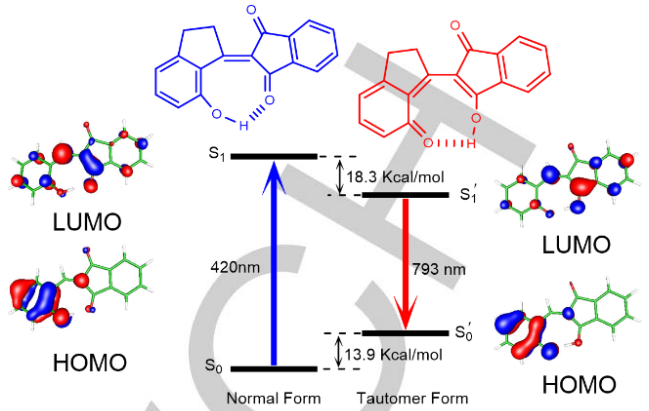

Figure 3. Relative energy of the normal and tautomer species for 8-HB-L1 in ground and excited states (in cyclohexane), calculated using B3LYP/6-31g* level. Also depicted are the calculated HOMO and LUMO for normal and tautomer species.

The rather low emission yield for **8-HB-L1** in cyclohexane leads us to propose dominant non-radiative decay channels for both normal and tautomer emissions. The femtosecond fluorescence upconversion measurements were then carried out to gain further insight into the relaxation properties of **8-HB-L1**. Upon 400 nm laser excitation and monitoring at either the blue (e.g. 500 nm) or red (e.g. 700 nm) emission region, both corresponding emissions revealed system limited response of ~220 fs (see Figure S4 in Supporting Information). The results, on the one hand, indicate an ultrafast (< 220 fs) ESIPT for **8-HB-L1** in cyclohexane, similar to that of the 7-MR H-bonding systems such as ***o*-HBDI**[10] and ***o*-LHBDI**,[11] giving an extremely weak normal emission. On the other hand, in sharp contrast to the exclusively tautomer emission observed in 5, 6 and 7-MR ESIPT molecules, the tautomer emission in **8-HB-L1** is also very weak, leading to simultaneous observation for both normal and tautomer emissions. The ultra-weak tautomer emission may be rationalized by its large exocyclic distortion. The results of calculation for **8-HB-L1** show that ∠C11–C10–C1–C2 angle changes largely from ~16.8° (normal form) to ~0° (tautomer form) during ESIPT (see Figure 4). Such a torsional motion associated with H-bond may play a key role to vastly deactivate the tautomer emission. This process may only require very small amplitude motion such as a slight bending associated with H-bond, which seems to be operative in the solid as well because very weak emission was observed for **8-HB-L1** in the solid powder. Nevertheless, as shown in Figure 2 the ~700 nm proton-transfer tautomer emission is obviously resolvable.

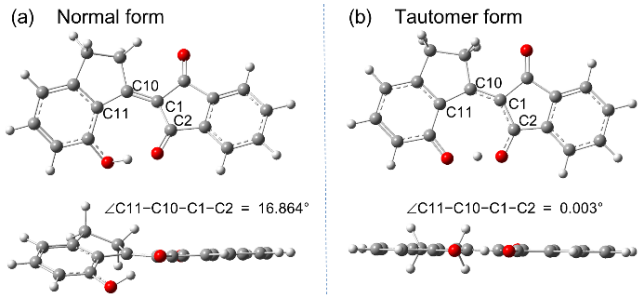

Figure 4. The front and side views of DFT optimized geometries for (a) normal of **8-HB-L1** in the S_0 ground state and (b) tautomer forms of **8-HB-L1** in the S_1 excited state.

Conclusions

In conclusion, we have carried out a strategic design, synthesis and characterization of three potential 8-MR H-bonding systems. As a result, all titled molecules have been thoroughly examined by X-ray structure analyses, among which a structurally locked **8-HB-L1** is proved to be in an 8-MR H-bonding configuration per se, while the flexible molecules **8-HB-1** and **8-HB-2** failed to render 8-MR intramolecular H-bond due to their high steric hindrance. While ESIPT takes place in **8-HB-L1**, the resulting tautomer emission is subject to dominant non-radiative deactivation, induced perhaps by the structure deformation that couples with the H-bonding motion or touches the conical intersection.[15] By and large, the results demonstrate for the first time a successful synthetic route to attain an 8-MR molecule **8-HB-L1**, which so far possesses the highest atom numbers involved in the intramolecular H-bond ring, adding a new family to the π-conjugated intramolecular H-bonding systems.

Experimental Section

Instrumentation and Materials

NMR spectra were recorded on Varian Unity 400. High resolution mass spectra were recorded by Gas Chromatograph-Mass Spectrometer (Finnigan MAT TSQ-46C GC/MS/MS/DS). The X-ray diffraction intensity data were collected at 200 K or 150 K on a Rigaku RAXIS RAPID IP imaging plate system with MoKα radiation (λ = 0.71073 Å). UV-visible absorption spectra were recorded by a Hitachi (U-3310) spectrophotometer, and steady-state emission spectra were taken from an Edinburgh (FS920) fluorimeter. Ultrafast dynamics was studied by the femtosecond fluorescence up-conversion (FOG100, CDP). Commercially available reagents and solvents were used without further purification.

Synthesis of 2-(2-hydroxybenzylidene)-2H-indene-1,3-dione (8-HB-1)

According to literature procedure,[14] **8-HB-1** was prepared as a yellow solid. ^{1}H NMR (400 MHz, $CDCl_3$): δ 9.61 (s, 1H), 8.04-8.02 (m, 3H), 7.87–7.80 (m, 4H), 7.49–7.45 (m, 1H), 7.07 (d, J = 8.0 Hz, 1H), 7.01 (t, J = 8.0 Hz, 1H).

Synthesis of (E)-3-(phenylimino)-2,3-dihydro-1H-inden-4-ol (PDI)

To a solution of 7-hydroxy-1-indanone (100 mg, 0.61 mmol) and aniline (57 mg, 0.61 mmol) in ethanol (30 mL), a few drops of formic acid was added. Then the mixture was stirred at 80 ºC for 6 h. The mixture was evaporated under vacuum. The crude product was purified by flash chromatography eluting with 1:5 EtOAc/hexane to afford PDI (120 mg, 88%) as yellow solid. ^{1}H NMR (400 MHz, $CDCl_3$): δ 11.08 (br, 1H), 7.41–7.32 (m, 3H), 7.19–7.15 (m, 1H), 7.06–7.03 (m, 2H), 6.87–6.81 (m, 2H), 3.08 (t, J = 6.0 Hz, 2H), 2.81–2.78 (m, 2H). ^{13}C NMR (100 MHz, $CDCl_3$): δ 178.12, 157.64, 150.29, 149.04, 133.80, 128.86, 124.41, 123.69, 120.87, 115.78, 113.08, 29.33, 28.42. MS (EI, 70 eV): m/z (relative intensity) 223 (M+, 100); HRMS calcd. for $C_{15}H_{13}NO$ 223.0997, found 223.1002.

Synthesis of 7-hydroxy-2,3-dihydro-[1,2'-biindenylidene]-1',3'-dione (8-HB-L1)

A solution of **PDI** (30 mg, 0.13 mmol) and 1,3-indan-dione (20 mg, 0.13 mmol) in acetonitrile (30 mL) was stirred at 80 ºC for 6 h. The mixture was evaporated under vacuum. The crude product was purified by flash chromatography eluting with 1:6 EtOAc/hexane to afford **8-HB-L1** (12 mg, 33%) as orange solid. ^{1}H NMR (400 MHz, $CDCl_3$): δ 10.78 (s, 1H), 7.96–7.89 (m, 2H), 7.79–7.74 (m, 2H), 7.51–7.47 (m, 1H), 7.01–6.95 (m, 2H), 3.77–3.75 (m, 2H), 3.11 (t, J = 5.6 Hz, 2H). ^{13}C NMR (100 MHz, $CDCl_3$): δ 195.51, 191.65, 171.67, 159.58, 157.54, 140.67, 140.28, 137.31, 135.63, 134.59, 128.88, 123.54, 122.72, 121.35, 118.98, 117.25, 38.26, 31.53. MS (EI, 70 eV): m/z (relative intensity) 276 (M+, 100); HRMS calcd. for $C_{18}H_{12}O_3$ 276.0786, found 276.0781.

Synthesis of 1-(2-bromocyclopent-1-en-1-yl)-2-methoxybenzene (1)

Under an nitrogen atmosphere, to a solution of 1,2-dibromocyclopent-1-ene (300 mg, 1.33 mmol), (2-methoxyphenyl)boronic acid (201 mg, 1.33 mmol),[16] and Na_2CO_3 (1.4 mL, 2 M, 2.66 mmol) in toluene/ethanol (30 mL:7.5 mL), Pd(PPh3)4 (77 mg, 0.06 mmol) was added. The resulting mixture was stirred at 100 ºC for 12 h. After cooling to room temperature, the solution was evaporated under vacuum. The residue was extracted sequentially with water (10 mL), CH_2Cl_2 (3 × 10 mL), dried ($MgSO_4$) and evaporated under vacuum. The crude product was purified by flash chromatography eluting with 1:4 EtOAc/hexane to afford 1 (204 mg, 61%) as white solid. ^{1}H NMR (400 MHz, $CDCl_3$): δ 7.29–7.22 (m, 2H), 6.97–6.93 (m, 1H), 6.88 (d, J = 8.0 Hz, 1H), 3.82 (s, 3H), 2.83–2.78 (m, 2H), 2.74–2.69 (m, 2H), 2.09–2.02 (m, 2H). ^{13}C NMR (100 MHz, $CDCl_3$): δ 156.21, 138.49, 129.86, 128.42, 125.48, 119.87, 117.85, 110.62, 55.50, 41.03, 36.18, 22.78. MS (EI, 70 eV): m/z (relative intensity) 252 (M+, 100); HRMS calcd. for $C_{12}H_{13}BrO$ 252.0150, found 252.0156.

Synthesis of 2-(2-(2-methoxyphenyl)cyclopent-1-en-1-yl)pyridine (2)

Under a nitrogen atmosphere, to a solution of compound 1 (100 mg, 0.4 mmol), 2-(tributylstannyl)pyridine[17] (189 mg, 0.48 mmol) in toluene (30 mL), $Pd(PPh_3)_4$ (23 mg, 0.02 mmol) was added. The reaction mixture was refluxed for 12 h, and then the solution was evaporated under vacuum. The crude product purified by flash chromatography eluting with 1:4 EtOAc/hexane to afford 2 (70 mg, 70%) as white solid. ^{1}H NMR (400 MHz, $CDCl_3$): δ 8.52–8.50 (m, 1H), 7.30–7.20 (m, 2H), 7.01–6.94 (m, 2H), 6.87–6.91 (m, 3H), 3.69 (s, 3H), 3.09–3.05 (m, 2H), 2.90–2.85 (m, 2H), 2.10–2.04 (m, 2H). ^{13}C NMR (100 MHz, $CDCl_3$): δ 156.79, 148.65, 140.26, 138.66, 135.07, 129.87, 128.40, 128.09, 122.79, 120.85, 120.73(×2), 110.06, 55.29, 39.89, 36.25, 22.36. MS (EI, 70 eV): m/z (relative intensity) 251 (M+, 100); HRMS calcd. for $C_{17}H_{17}NO$ 251.1310, found 251.1303.

Synthesis of 2-(2-(pyridin-2-yl)cyclopent-1-en-1-yl)phenol (8-HB-2)

Under a nitrogen atmosphere, to a solution of compound 2 (60 mg, 0.24 mmol) in dried CH_2Cl_2 (20 mL) at 0 ºC, BBr_3 (0.31 mL, 1M, 0.31 mmol) was added slowly with a syringe. After stirring for 6 h, the solution was evaporated under vacuum. The residue was extracted sequentially with water (10 mL), CH_2Cl_2 (3 × 10 mL), dried ($MgSO_4$) and evaporated under vacuum. The crude product purified by flash chromatography eluting with 1:2 EtOAc/hexane to afford **8-HB-2** (32 mg, 56%) as white solid. ^{1}H NMR (400 MHz, $CDCl_3$): δ 12.01 (br, 1H), 8.43 (d, J = 5.2 Hz, 1H), 7.71–7.66 (m, 1H), 7.32 (d, J = 8.0 Hz, 1H), 7.18–7.04 (m, 4H), 6.86–6.82 (m, 1H), 3.04–3.01 (m, 2H), 3.00–2.88 (m, 2H), 2.11–2.04 (m, 2H). ^{13}C NMR (100 MHz, CDCl3): δ 155.43, 154.74, 146.70, 140.39, 137.49, 135.44, 128.83, 128.49, 128.19, 122.49, 121.45, 120.40, 119.89, 43.02, 37.79, 22.69. MS (EI, 70eV): m/z (relative intensity) 237 (M+, 100); HRMS calcd. for C16H15NO 237.1154, found 237.1146.

Computational Methodology

The density functional theory (DFT) method was utilized to optimize the geometries of the singlet ground states, and time-dependent density functional theory (TDDFT) methodology was employed to calculate the excited-state structures and related optical properties of all molecules with a B3LYP hybrid function in combination with a polarizable continuum model (PCM) in cyclohexane. The 6-31+G(d,p) basis set was employed for all atoms.[18]

Acknowledgements

P.T.C. thanks the Ministry of Science and Technology, Taiwan for financial support.

Keywords: proton transfer • hydrogen bonds • single crystal • fluorescence • eight-membered ring

[1] a) J. E. Kwon, S. Y. Park, *Adv. Mater.* **2011**, *23*, 3615-3642; b) J. Zhao, S. Ji, Y. Chen, H. Guo, P. Yang, *Phys. Chem. Chem. Phys.* **2012**, *14*, 8803-8817; c) A. P. Demchenko, K.-C. Tang, P.-T. Chou, *Chem. Soc. Rev.* **2013**, *42*, 1379-1408; d) V. I. Tomin, A. P. Demchenko, P.-T. Chou, *J. Photochem. Photobiol. C: Photochem. Rev.* **2015**, *22*, 1-18.

[2] a) P. K. Sengupta, M. Kasha, *Chem. Phys. Lett.* **1979**, *68*, 382-385; b) P. Chou, D. McMorrow, T. J. Aartsma, M. Kasha, *J. Phys. Chem.* **1984**, *88*, 4596-4599.

[3] a) W.-S. Yu, C.-C. Cheng, Y.-M. Cheng, P.-C. Wu, Y.-H. Song, Y. Chi, P.-T. Chou, *J. Am. Chem. Soc.* **2003**, *125*, 10800-10801; b) T.-Y. Lin, K.-C. Tang, S.-H. Yang, J.-Y. Shen, Y.-M. Cheng, H.-A. Pan, Y. Chi, P.-T. Chou, *J. Phys. Chem. A.* **2012**, *116*, 4438-4444; c) Y. Chi, B. Tong, P.-T. Chou, *Coord. Chem. Rev.* **2014**, *281*, 1-25.

[4] a) S. Barman, S. K. Mukhopadhyay, S. Biswas, S. Nandi, M. Gangopadhyay, S. Dey, A. Anoop, N. D. Pradeep Singh, *Angew. Chem. Int. Ed.*, **2016**, *55*, 4194-4198; b) B. Bhattacharya, A. Halder, L. Paul, S. Chakrabarti, D. Ghoshal, *Chem. Eur. J.*, **2016**, *22*, 14998-15005; c) J. Cheng, D. Liu, L. Bao, K. Xu, Y. Yang, K. Han, *Chem. Asian J.,* **2014**, *9*, 3215-3220; d) X. Wang, Z.-Z. Li, S.-F. Li, H. Li, J. Chen, Y. Wu, H. Fu, *Adv. Opt. Mater.*, **2017**, *5*, 1700027; e) W. Zhang, Y. Yan, J. Gu, J. Yao, Y. S. Zhao, *Angew. Chem. Int. Ed.*, **2015**, *54*, 7125-7129; f) M. Tasior, V. Hugues, M. Blanchard-Desce, D. T. Gryko, *Chem. Asian J.,***2012**, *7*, 2656-2661; g) C. Zhao, X. Li, F. Wang, *Chem. Asian J.,* **2014**, *9*, 1777-1781.

[5] a) J. Heldt, D. Gormin, M. Kasha, *Chem. Phys.* **1989**, *136*, 321-334; b) M. L. Martinez, S. L. Studer, P. T. Chou, *J. Am. Chem. Soc.* **1991**, *113*, 5881-5883; c) S. M. Andrade, S. M. B. Costa, *Phys. Chem. Chem. Phys.* **1999**, *1*, 4213-4218; d) J. Wakita, S. Inoue, N. Kawanishi, S. Ando, *Macromolecules* **2010**, *43*, 3594-3605.

[6] a) M. L. Martinez, W. C. Cooper, P.-T. Chou, *Chem. Phys. Lett.* **1992**, *193*, 151-154; b) K.-Y. Chen, C.-C. Hsieh, Y.-M. Cheng, C.-H. Lai, P.-T. Chou, *Chem. Commun.* **2006**, 4395-4397; c) J. Piechowska, D. T. Gryko, *J. Org. Chem.* **2011**, *76*, 10220-10228; d) J. Piechowska, K. Virkki, B. Sadowski, H. Lemmetyinen, N. V. Tkachenko, D. T. Gryko, *J. Phys. Chem. A.* **2014**, *118*, 144-151.

[7] a) A. Heller, D. L. Williams, *J. Phys. Chem.* **1970**, *74*, 4473-4480; b) W. Frey, F. Laermer, T. Elsaesser, *J. Phys. Chem.* **1991**, *95*, 10391-10395; c) J. Seo, S. Kim, Y.-S. Lee, O.-H. Kwon, K. H. Park, S. Y. Choi, Y. K. Chung, D.-J. Jang, S. Y. Park, *J. Photochem. Photobiol. A: Chem* **2007**, *191*, 51-58; d) S. Park, J. E. Kwon, S. Y. Park, *Phys. Chem. Chem. Phys.* **2012** *14*, 8878-8884; e) T. Shida, T. Mutai, K. Araki, *CrystEngComm* **2013**, *15*, 10179-10182.

[8] a) G. Wiosna, I. Petkova, M. S. Mudadu, R. P. Thummel, J. Waluk, *Chem. Phys. Lett.* **2004**, *400*, 379-383; b) Z. Zhang, Y.-H. Hsu, Y.-A. Chen, C.-L. Chen, T.-C. Lin, J.-Y. Shen, P.-T. Chou, *Chem. Commun.* **2014**, *50*, 15026-15029.

[9] T. Arai, M. Moriyama, K. Tokumaru, *J. Am. Chem. Soc.*, **1994**, *116*, 3171-3172.

[10] K.-Y. Chen, Y.-M. Cheng, C.-H. Lai, C.-C. Hsu, M.-L. Ho, G.-H. Lee, P.-T. Chou, *J. Am. Chem. Soc.* **2007**, *129*, 4534-4535.

[11] Y.-H. Hsu, Y.-A. Chen, H.-W. Tseng, Z. Zhang, J.-Y. Shen, W.-T. Chuang, T.-C. Lin, C.-S. Lee, W.-Y. Hung, B.-C. Hong, S.-H. Liu, P.-T. Chou, *J. Am. Chem. Soc.* **2014**, *136*, 11805-11812.

[12] a) X. Li, Y.-D. Wu, D. Yang, *Acc. Chem. Res.* **2008**, *41*, 1428-1438; b) X. Li, D. Yang, *Chem. Commun.* **2006**, 3367-3379.

[13] C.-C. Hsieh, P.-T. Chou, C.-W. Shih, W.-T. Chuang, M.-W. Chung, J. Lee, T. Joo, *J. Am. Chem. Soc.* **2011**, *133*, 2932-2943.

[14] P. Yang, Q. Zhang, W. Sun, *Res. Chem. Intermed.* **2012**, *38*, 1063-1068.

[15] G. A. Parada, T. F. Markle, S. D. Glover, L. Hammarström, S. Ott, B. Zietz, *Chem. Eur. J.*, **2015**, *21*, 6362-6366.

[16] M. Iwao, T. Takeuchi, N. Fujikawa, T. Fukuda, F. Ishibashi, *Tetrahedron Letters* **2003**, *44*, 4443-4446.

[17] T. N. Y. Hoang, M. Humbert-Droz, T. Dutronc, L. Guénée, C. Besnard, C. Piguet, *Inorg. Chem.*, **2013**, *52*, 5570-5580.

[18] M. J. Frisch, G. W. Trucks, H. B. Schlegel, G. E. Scuseria, M. A. Robb, J. R. Cheeseman, J. A. Montgomery, Jr., T. Vreven, K. N. Kudin, J. C. Burant, J. M. Millam, S. S. Iyengar, J. Tomasi, V. Barone, B. Mennucci, M. Cossi, G. Scalmani, N. Rega, G. A. Petersson, H. Nakatsuji, M. Hada, M. Ehara, K. Toyota, R. Fukuda, J. Hasegawa, M. Ishida, T. Nakajima, Y. Honda, O. Kitao, H. Nakai, M. Klene, X. Li, J. E. Knox, H. P. Hratchian, J. B. Cross, V. Bakken, C. Adamo, J. Jaramillo, R. Gomperts, R. E. Stratmann, O. Yazyev, A. J. Austin, R. Cammi, C. Pomelli, J. W. Ochterski, P. Y. Ayala, K. Morokuma, G. A. Voth, P. Salvador, J. J. Dannenberg, V. G. Zakrzewski, S. Dapprich, A. D. Daniels, M. C. Strain, O. Farkas, D. K. Malick, A. D. Rabuck, K. Raghavachari, J. B. Foresman, J. V. Ortiz, Q. Cui, A. G. Baboul, S. Clifford, J. Cioslowski, B. B. Stefanov, G. Liu, A. Liashenko, P. Piskorz, I. Komaromi, R. L. Martin, D. J. Fox, T. Keith, M. A. Al-Laham, C. Y. Peng, A. Nanayakkara, M. Challacombe, P. M. W. Gill, B. Johnson, W. Chen, M. W. Wong, C. Gonzalez, J. A. Pople, *Gaussian 09*, Revision A.02,; Gaussian, Inc.: Wallingford CT, 2009.. .

10.1002/asia.201701057

Entry for the Table of Contents (Please choose one layout)

Layout 1:

FULL PAPER

In searching for seminal eight-membered ring π-conjugated hydrogen bonding (8-MR H-bonding) systems we strategically designed and synthesized a series of compounds (**8-HB-1**, **8-HB-L1**, **8-HB-2**) potentially possessing 8-MR H-bond, among which the structurally locked **8-HB-L1** is affirmed to be the authentic 8-MR H-bonding system with prominent excited-state intramolecular proton transfer.

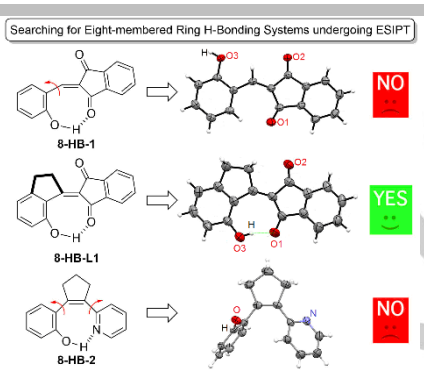

Fan-Yi Meng, Yen-Hao Hsu, Zhiyun Zhang, Pei-Jhen Wu, Yi-An Chen, Yi-Ting Chen, Chi-Lin Chen, Chi-min Chao, Kuan-Miao Liu, Pi-Tai Chou**

Page No. – Page No.

The Quest of Excited-State Intramolecular Proton Transfer via Eight-Membered Ring π-Conjugated Hydrogen Bonding System

Layout 2:

FULL PAPER

((Insert TOC Graphic here; max. width: 11.5 cm; max. height: 2.5 cm))

*Author(s), Corresponding Author(s)**

Page No. – Page No.

Title

Text for Table of Contents